Molecular Dynamics of Proteins with the OPLS Potential Functions. Simulation of the Third Domain of Silver Pheasant Ovomucoid in Water

Julian Tirado-Rives and William L. Jorgensen*

Contribution from the Department of Chemistry, Purdue University, West Lafayette, Indiana 47907. *Received May 15, 1989*

Abstract: A molecular dynamics simulation using the OPLS nonbonded potential functions has been carried out for the third domain of silver pheasant ovomucoid in aqueous solution. Insights have been obtained on the quality of the force field, the convergence of such calculations, differences in the protein's structure in the crystal and in aqueous solution, protein hydration, and the dynamics of water molecules near a protein. The simulation covered 100 ps at 25 °C, which allowed complete equilibration prior to averaging and analysis of the results. Continuous monitoring of the potential energy, root-mean-square deviations from the crystal structure, and other properties indicated that convergence to a stable structure was achieved after 30–40 ps. The RMS deviation of the instantaneous structure from the crystal structure after 100 ps is 1.43 Å for the backbone atoms of residues 8–56 and 1.61 Å for all residues. There is substantial reorganization of hydrogen bonds that do not involve secondary structure in comparing the crystal and solution structures, though in the simulation Ala-44 is displaced from the α-helix and Lys-29, Thr-30, Tyr-31, and Gly-32 are moved out of hydrogen-bonding distance in the triple-stranded antiparallel β-sheet. Analyses of the protein–water hydrogen bonding were also carried out and are compared with results from previous simulations and NMR experiments.

The rational design or modification of biomolecules, including the development of selective inhibitors for enzymes, requires detailed knowledge of the structure, dynamics, and corresponding energetics. Importantly, the continuous improvement of crystallographic techniques has made possible the precise determination of the structures of many proteins, as reflected in the more than 300 entries now deposited in the Brookhaven Protein Data Bank.[1] However, the structures obtained in this fashion represent an ordered crystalline state, while biological processes normally occur in solution. Furthermore, the data obtained from crystal structures are static in nature, although some dynamic information can be obtained from the temperature (*B*) factors.[2] Recent advances in nuclear magnetic resonance spectroscopy (NMR), particularly the use of 2-D nuclear Overhauser effects, have been very valuable, since sets of distance constraints are obtained that can be transformed into three-dimensional structures of proteins in solution.[3] Although this methodology allows the direct observation of proteins in their native solution state, the structures obtained reflect conformational averaging and are not unique solutions for the data sets. Nevertheless, the combination of the experimental structural results with molecular dynamics (MD) calculations is proving to be a powerful approach to the detailed characterization of the structure, dynamics, and energetics of proteins.[4]

Since the pioneering MD simulation of bovine pancreatic trypsin inhibitor (BPTI) in vacuo,[5] there have been numerous molecular dynamics calculations of proteins.[4] However, the aqueous medium has rarely been represented in molecular detail. Some exceptions are for BPTI,[6-8] avian pancreatic polypeptide hormone (APP),[9] and parvalbumin[10] in aqueous solution and BPTI in its full crystalline environment.[11] Other recent calculations have been more focused toward the modeling of enzyme–inhibitor complexes in water, including trypsin–benzamidine[12] and thermolysin–phosphonamidate.[13]

With the exceptions of the parvalbumin[10] and one of the BPTI calculations,[8] all of these simulations were run for very short times. Total times including the equilibrium periods were 15–30 ps for some of the BPTI and the APP simulations and 45 ps for the trypsin–benzamidine complex, as compared to 106 and 210 ps for the parvalbumin and the longest of the BPTI calculations, respectively. It is not clear that the shorter simulation times allow the systems to achieve equilibrium and to remove the biases from the starting conformation, typically obtained from a crystal structure. In this setting, the present study was undertaken to follow a molecular dynamics simulation for a protein in water for a long enough time to assess the convergence issue, to further test the performance of the OPLS force field,[14] and to obtain insights on protein hydration and possible differences between the solution and crystal structures. The protein selected for the study was the third domain of silver pheasant ovomucoid (OMSVP3).[15]

Ovomucoids make up about 10% of the protein in avian egg whites, in which they are the dominant inhibitors of serine proteases. They are members of the Kazal family of pancreatic secretory inhibitors, which are generally important in controlling the premature activation of pancreatic zymogens. The complete ovomucoid consists of three homologous, tandem domains, each

(1) Bernstein, F. C.; Koetzle, T. F.; Williams, G. J. B.; Meyer, E. F., Jr.; Brice, M. D.; Rodgers, J. R.; Kennard, O.; Shimanouchi, T.; Tasumi, M. *J. Mol. Biol.* **1977**, *112*, 535.
(2) Petsko, G. A.; Ringe, D. *Annu. Rev. Biophys. Bioeng.* **1984**, *13*, 331. Fraunfelder, H.; Hartmann, H.; Karplus, M.; Kuntz, I. D., Jr.; Kuriyan, J.; Parak, F.; Petsko, G. A.; Ringe, D.; Tilton, R. A., Jr.; Connolly, M. L.; Max, N. *Biochemistry* **1987**, *26*, 254.
(3) Wüthrich, K. *NMR of Proteins and Nucleic Acids*; John Wiley & Sons: New York, 1986.
(4) For recent reviews, see: (a) Karplus, M.; McCammon, J. A. *CRC Crit. Rev. Biochem.* **1986**, *9*, 293. (b) McCammon, J. A.; Harvey, S. C. *Dynamics of Proteins and Nucleic Acids*; Cambridge University Press: Cambridge, England, 1987.
(5) McCammon, J. A.; Gelin, B. R.; Karplus, M. *Nature* **1977**, *267*, 585.
(6) van Gunsteren, W. F.; Berendsen, H. J. C. *J. Mol. Biol.* **1984**, *176*, 559.
(7) Ghosh, I.; McCammon, J. A. *J. Phys. Chem.* **1987**, *91*, 4878.
(8) Levitt, M.; Sharon, R. *Proc. Natl. Acad. Sci. U.S.A.* **1988**, *85*, 7557.
(9) Krüger, P.; Straßburger, W.; Wollmer, A.; van Gunsteren, W. F. *Eur. Biophys. J.* **1985**, *13*, 77.
(10) (a) Ahlström, P.; Teleman, O.; Jönsson, B.; Forsén, S. *J. Am. Chem. Soc.* **1987**, *109*, 1541. (b) Ahlström, P.; Teleman, O.; Jönsson, B. *J. Am. Chem. Soc.* **1988**, *110*, 4198.
(11) (a) van Gunsteren, W. F.; Karplus, M. *Biochemistry* **1982**, *21*, 2259. (b) Swaminathan, S.; Ichiye, T.; van Gunsteren, W. F.; Karplus, M. *Biochemistry* **1982**, *21*, 5230. (c) van Gunsteren, W. F.; Berendsen, H. J. C.; Hermans, J.; Hol, W. G. J.; Postma, J. P. M. *Proc. Natl. Acad. Sci. U.S.A.* **1983**, *80*, 4315.
(12) Wong, C. F.; McCammon, J. A. *Isr. J. Chem.* **1986**, *27*, 211; *J. Am. Chem. Soc.* **1986**, *108*, 3830.
(13) Bash, P. A.; Singh, U. C.; Brown, F. K.; Langridge, R.; Kollman, P. A. *Science* **1987**, *235*, 574.
(14) Jorgensen, W. L.; Tirado-Rives, J. *J. Am. Chem. Soc.* **1988**, *110*, 1657.
(15) A preliminary report on this work was provided in the Proceedings of the 1988 Nobel Symposium: Jorgensen, W. L.; Tirado-Rives, J. *Chem. Scr.* **1989**, *29A*, 191.

0002-7863/90/1512-2773$02.50/0

of which may inhibit a protease. The third domain contains 56 amino acid residues that can be detached by controlled proteolysis. These fragments are typically at least as active as the full ovomucoid.

Sequences have now been determined for ovomucoid third domains from over 100 avian species by Laskowski and coworkers.[16] They have also determined association constants for many of these inhibitors with α-chymotrypsin (AC), elastase (HLE), subtilisin, and *Streptomyces griseus* proteases A and B (SGPA and SGPB).[17,18] Many of the sequences differ by only one or a few residue changes, so an unusually complete structure/activity data base is being constructed.

Besides the association and hydrolytic constants, some structural data are also available. Crystal structures have been determined for complexes of turkey ovomucoid third domain with SGPB,[19] HLE,[20] and AC,[21] for two isolated third domains, silver pheasant[22] and Japanese quail,[23] and for their corresponding hydrolyzed forms.[24] However, structural data in solution are limited to two studies by 2-D NMR, specifically, for turkey ovomucoid third domain in both its native[25] and hydrolyzed forms.[26]

The typical structure of an ovomucoid third domain contains three disulfide bridges, a 10–11 residue long α-helix, and a triple-stranded antiparallel β-sheet. The combination of small size, a large body of experimental data, and interesting structure makes the ovomucoids unusually attractive for a series of molecular dynamics investigations. Such simulations could provide detailed structural and thermodynamic information, which would be of great assistance in the interpretation of the biophysical data and the development of selective inhibitors. The third domain of silver pheasant ovomucoid was chosen for this initial study owing to its greater sequence homology with other ovomucoids and the better resolution of its crystal structure than that of Japanese quail.

Computational Procedure

The entire simulation was conducted on Sun-4 computers using the AMBER 3.0 program,[27] with minor local modifications to improve its use of the UNIX environment. The OPLS nonbonded parameters[14] were used for the protein atoms in conjuction with the TIP3P model for water.[28] As specified in the OPLS model, the dielectric constant was kept fixed at 1.0, and the scaling factors for the 1,4-nonbonded interactions were 8.0 for the Lennard-Jones and 2.0 for the electrostatic interactions.[14] The energetics for angle bending and torsional motion were described with the AMBER united-atom force field.[27] During the simulation, all bond lengths and the H–H distances in water were kept constant by using the SHAKE algorithm[29] with a tolerance of 0.0004 Å, which allowed the use of a time step of 2 fs. The temperature and pressure were kept constant at 298 K and 1 bar (0.987 atm). A nonbonded pair list was used to accelerate the calculations and was updated every 10 steps. This list was generated by using a residue-based cutoff (9 Å) to avoid splitting dipoles. All the calculations utilized periodic boundary conditions to avoid edge effects.

The initial coordinates for the third domain of silver pheasant ovomucoid were obtained from the crystal structure[22] deposited in the Brookhaven Protein Data Bank.[1,30] The protein molecule, without any of the crystallographically located water molecules, was centered in a rectangular box of water obtained by periodic translations in the x, y, and z directions of a cube of water previously equilibrated via Monte Carlo calculations. Any water molecule closer than 1.5 Å to any protein atom or farther away than 6 Å from the closest protein atom in any one Cartesian direction was then deleted to give an initial system containing the solute plus 1721 water molecules (5676 total atoms) in a rectangular box of dimensions 43.8 × 42.0 × 34.3 Å.

The initial preparation of the system consisted of 100 steps of steepest descent energy minimization, followed by a short (1 ps) constant volume molecular dynamics run. The resulting structure was then used as the starting point for the MD simulation at constant temperature and pressure. Initial atomic velocities were assigned from a Maxwellian distribution corresponding to a temperature of 298 K. The values of the potential energy, RMS deviation from the crystal structure, and volume were monitored continuously in order to follow the equilibration of the system. A total time of 100 ps was covered in the simulation, during which the coordinates, velocities, and energies were saved every 50 time steps (0.1 ps) for further analysis.

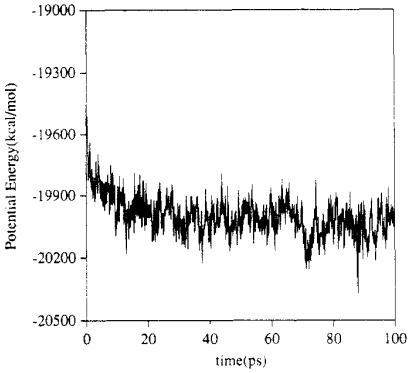

Figure 1. Potential energy variation during the course of the MD simulation.

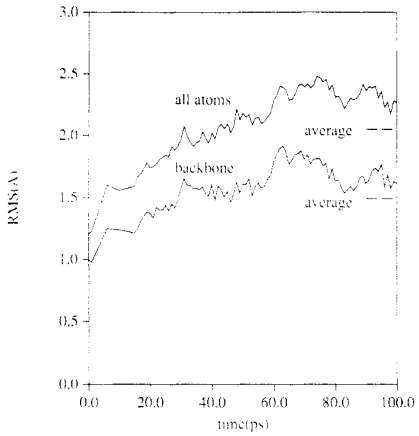

Figure 2. RMS deviations between the instantaneous computed structure and the crystal structure for all residues as a function of simulation time.

Results

Convergence Behavior. The potential energy and RMS deviations of the main-chain atoms (N, C^{α}, C, and O) of residues 8–56 for each instantaneous structure are plotted in Figures 1 and 2, respectively, as a function of simulation time. The first seven

(16) Laskowski, M., Jr.; Kato, I.; Ardelt, W.; Cook, J.; Denton, A.; Empie, M. W.; Kohr, W. J.; Park, S. J.; Parks, K.; Schatzley, B. L.; Schoenberger, O. L.; Tashiro, M.; Vichot, G.; Whatley, H. E.; Wieczorek, A.; Wieczorek, M. *Biochemistry* **1987**, *26*, 202. Kato, I.; Kohr, W. J.; Laskowski, M., Jr. *Biochemistry* **1987**, *26*, 193.
(17) Empie, M. W.; Laskowski, M., Jr. *Biochemistry* **1987**, *21*, 2274.
(18) Laskowski, M., Jr.; Tashiro, M.; Empie, M. W.; Park, S. J.; Kato, I.; Ardelt, W.; Wieczorek, M. In *Proteinase Inhibitors: Medical and Biological Aspects*; Katunuma, N., Umezawa, H., Hozer, H., Eds.; Japan Scientific Societies Press: Tokyo, 1983; p 55.
(19) Fujinaga, M.; Read, R.; Sielecki, A. R.; Ardelt, W.; Laskowski, M., Jr.; James, M. N. G. *Proc. Natl. Acad. Sci. U.S.A.* **1982**, *79*, 4868. Read, R.; Fujinaga, M.; Sielecki, A. R.; James, M. N. G. *Biochemistry* **1983**, *22*, 4420.
(20) Bode, W.; Wei, A.-Z.; Huber, R.; Meyer, E.; Travis, J.; Neumann, S. *EMBO J.* **1986**, *10*, 2453.
(21) Read, R.; Fujinaga, M.; Sielecki, A. R.; Ardelt, W.; Laskowski, M., Jr. *Acta Crystallogr., Sect. A, Suppl.* **1984**, *40*, C-50.
(22) Bode, W.; Epp, O.; Huber, O.; Laskowski, M., Jr.; Ardelt, W. *Eur. J. Biochem.* **1985**, *147*, 387.
(23) Weber, E.; Papamokos, E.; Bode, W.; Huber, R.; Kato, I.; Laskowski, M., Jr. *J. Mol. Biol.* **1981**, *149*, 109. Papamokos, E.; Weber, E.; Bode, W.; Huber, R.; Empie, M. W.; Kato, I.; Laskowski, M., Jr. *J. Mol. Biol.* **1982**, *158*, 515.
(24) Musil, D.; Bode, W.; Mayr, I.; Huber, R.; Laskowski, M., Jr.; Lin, T.-Y.; Ardelt, W. Unpublished results.
(25) Robertson, A.; Westler, W. M.; Markley, J. L. *Biochemistry* **1988**, *27*, 2519.
(26) Rhyu, G. I.; Markley, J. L. *Biochemistry* **1988**, *27*, 2529.
(27) Weiner, S. J.; Kollman, P. A.; Case, D. A.; Singh, U. C.; Ghio, C.; Alagona, G.; Profeta, S.; Weiner, P. J. *J. Am. Chem. Soc.* **1984**, *106*, 765.
(28) Jorgensen, W. L.; Chandrasekhar, J.; Madura, J. D.; Impey, R. W.; Klein, M. L. *J. Chem. Phys.* **1983**, *70*, 926.
(29) van Gunsteren, W. F.; Berendsen, H. J. C. *Mol. Phys.* **1977**, *34*, 1311.
(30) Entry 2OVO, version of Nov 8, 1985.

residues were excluded from the RMS deviations, since they form a pendant tail that is less well resolved in the crystal structure.[22] The RMS deviations are typically 0.2 Å higher when these residues are included. The system appears to have reached an equilibrium state after 30–40 ps, though the ultimate longevity of this state could only be determined in a much longer run. After this initial period, the simulation was continued to 100 ps in order to acquire enough data for averaging and analysis. In the 210-ps simulation for the other protease inhibitor, BPTI, in water, an equilibrium state was achieved after ca. 50 ps.[8]

Protein Structure and Dynamics. (A) Comparison with the Crystal Structure. The calculated mean structure of the protein in solution, obtained by directly averaging the Cartesian coordinates of all the saved structures from 30 to 100 ps, shows an RMS deviation from the crystal structure of 1.28 Å for the backbone atoms of residues 8–56 and 1.49 Å for all residues. Results from previous simulations in water include 1.05 Å for the C^{α} of APP, averaged from 5 to 15 ps,[9] and 0.77 Å for all the backbone atoms of residues 1–56 of BPTI, averaged from 105 to 210 ps.[8] Deviations from simulations in vacuo are typically larger by at least a factor of 2.[8,11]

The value of the RMS deviation of the instantaneous structure at 100 ps from the crystal structure is 1.43 Å for the backbone atoms of residues 8–56 and 1.61 Å for all residues. These values are in the same range as those obtained in previous, shorter simulations in water, e.g., 1.5 Å for only the C^{α} atoms of BPTI after 20 ps[6] and 1.72 Å for the C^{α} atoms of the trypsin–benzamidine complex at 45 ps.[12] Clearly, the AMBER/OPLS force field is providing a comparatively reasonable representation of the protein. An approximate base line for the RMS deviations can be deduced from the comparison of coordinates from proteins whose crystal structures have been solved in different crystalline forms or that have different molecules in the asymmetric unit. For five such cases, Chothia and Lesk obtained RMS deviations ranging from 0.25 to 0.40 Å, with a mean of 0.33 Å.[31]

A comparative plot of the backbone atoms of the crystal structure with the instantaneous structure at the end of the MD run is given in Figure 3. It can be seen that the tertiary structure is well preserved in the simulation. However, several striking differences with the crystal structure are revealed by more detailed graphical analyses:

(1) In the crystal structure, the amino acid side chains are mostly folded onto the surface of the protein, while in the solution simulation they extend more into the solvent. This effect likely reflects the lower water content in the crystal and the removal of the interprotein interactions. It also allows polar side chains to be better stabilized by hydration.

(2) The last residue of the α-helix in the crystal, Ser-44, does not form the required hydrogen bond with Ala-40 to be part of the helix in solution. This terminal hydrogen bond is also absent in the crystal structures of isolated Japanese quail[23] and hydrolyzed silver pheasant[24] ovomucoids and in the complexes of turkey ovomucoid with α-chymotrypsin[21] and *S. griseus* protease B.[19]

(3) As discussed in the next section, some of the residues of the outermost strand of the β-sheet (Lys-29, Thr-30, Tyr-31, and Gly-32) are tilted out of the plane of the other two strands in the simulation. This displacement inhibits the formation of the interstrand hydrogen bonds and yields greater hydrogen bonding between these residues and water molecules.

(4) The hydrogen bond in the crystal structure between the side chains of Glu-19 and Thr-17, which surround the scissile peptide bond between Met-18 and Glu-19, is not found in the simulation results. Instead, it is replaced by a hydrogen bond between the guanidinium fragment of Arg-21 and the carboxylate in Glu-19, while the hydroxyl group of Thr-17 is hydrogen-bonded to solvent molecules. This effect appears to be related to the loss of interprotein interactions. In the crystal lattice, the charged side charged side chain of Arg-21 is close to the carbonyl oxygens of Glu-10 and Pro-12 from a protein molecule in a neighboring unit cell. Interestingly, the same interprotein contacts were found in the crystal structure of Japanese quail ovomucoid, which has a very different crystalline form.[23,32] In addition, the Glu-19 carboxylate group in the crystal is hydrogen-bonded to the side-chain ammonium group of Lys-13 in the same neighboring cell. Figure 4 compares the different interactions in this region for the crystal structure and the instantaneous structure at 80 ps.

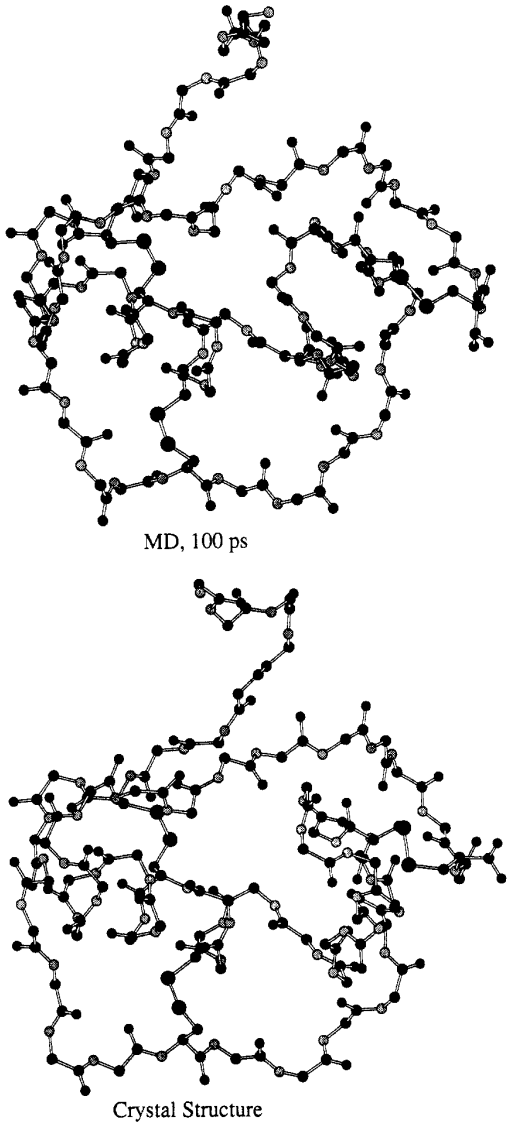

Figure 3. Comparison of backbone atoms in the instantaneous structure at the end of the simulation (t = 100 ps) and in the crystal structure.

The overall conformation of a protein can be expressed in terms of the backbone torsional angles ϕ_i (C_{i-1}–N_i–C_i^{α}–C_i) and ψ_i (N_i–C_i^{α}–C_i–N_{i+1}). The average values for these angles during the 30–100-ps period are compared with the corresponding values for the crystal structure in Figure 5. Consistent with the statements above, the biggest differences are found in the region around the C-terminus of the α-helix (Glu-43, Ser-44, and Asn-45), where the middle residue is twisted away from the helix, and in the region near the turn connecting the central and outer strands of the β-sheet (Ser-26, Asp-27, and Asn-28). Some of the other differences are of little consequence to the overall conformation, since compensation occurs when there are differences of opposing signs in an angle ψ_i and the subsequent ϕ_{i+1}. This is the case for Met-18 and Glu-19 and for the Thr-47, Leu-48, and Thr-49 region. The

(31) Chothia, C.; Lesk, A. M. *EMBO J.* **1986**, *5*, 823.

(32) Silver pheasant ovomucoid crystallizes in the $C2$ space group, while for Japanese quail, the crystals belong in the tetragonal $P4_12$ space group.

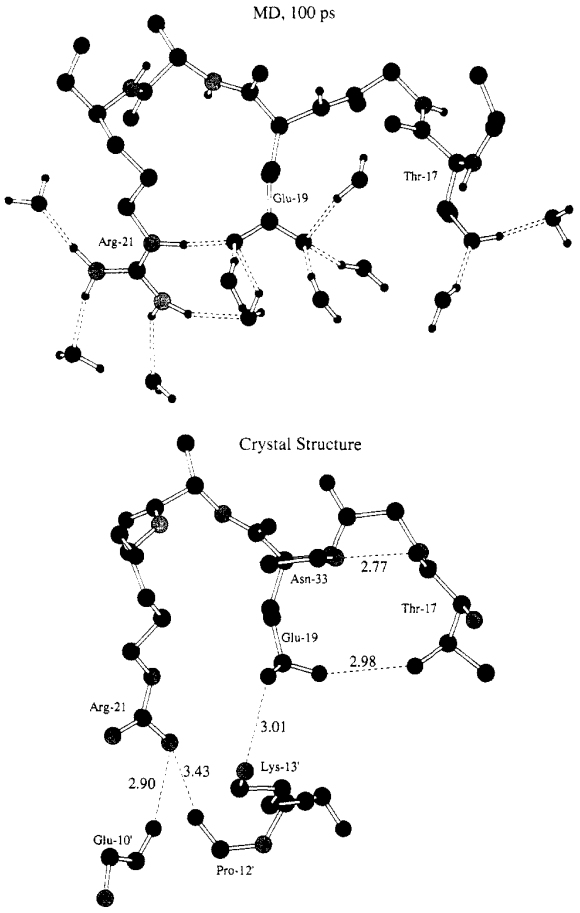

Figure 4. Hydrogen bonds near the scissile bond in the instantaneous structure at the end of the simulation (t = 100 ps) and in the crystal structure.

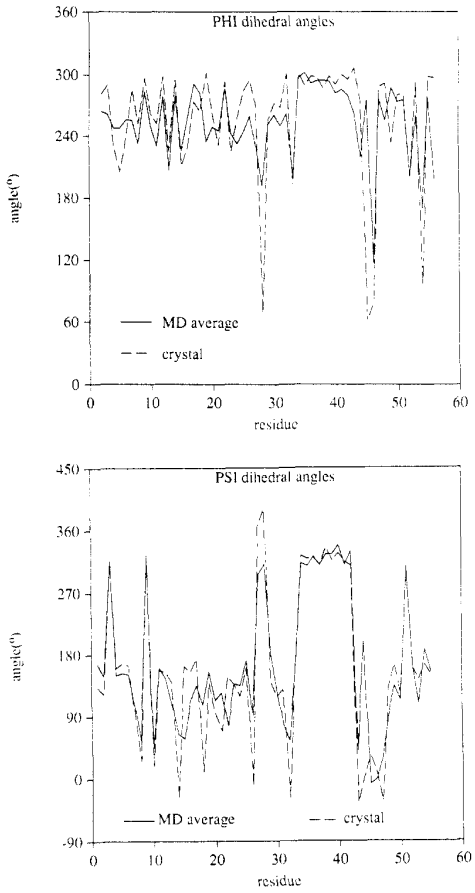

Figure 5. Plots of the backbone angles ϕ and ψ for the crystal structure and the averages from the MD simulation.

RMS differences from the crystal structure computed for each backbone dihedral angle over the entire protein are 39°, 48°, and 11° for ϕ, ψ, and ω, respectively. These differences are in the same range as the results from previous simulations, e.g., 31°, 37°, and 8° for ϕ, ψ, and ω in trypsin[12] and 26° and 33° for ϕ and ψ for BPTI in "van der Waals water".[11a]

A more global impression of the overall conformation of the protein can be obtained from the plots of ϕ vs ψ (Ramachandran maps) in Figure 6. The general trend observed in the maps is that residues in the α-helix stay close to the crystallographically observed angles, while those outside the helix are shifted toward values more typical of the C_5 and C_7^{eq} conformations. This displacement is consistent with the results of our previous energy-minimization studies on the conformations of *N*-acetylglycine-*N*-methylamide and *N*-acetylalanine-*N*-methylamide, which showed that these conformations are lower in energy than the corresponding α, α_R, or α_L alternatives.[14]

(B) Comparison with NMR Data. The NMR data in solution on native and hydrolyzed turkey ovomucoid should be relevant to the present case, since turkey and silver pheasant ovomucoids differ by only one residue (18: Met/Leu). In general, the main effort in the NMR investigations was devoted to the complete assignment of resonances, and only qualitative information regarding secondary structure was obtained.[25,26]

Although the principal conclusion of these studies was that the solution structure had to be very similar to that in the crystal, some details were explored further. In particular, the NOESY connectivities that establish the antiparallel triple-stranded β-sheet were given. Figure 7 provides a comparison of the segments comprising the β-sheet in the crystal and in the mean calculated solution structure, obtained by direct averaging of the Cartesian coordinates from 30 to 100 ps in the MD simulation. The interproton distances given with the crystal fragments are measured in the crystal[33] but correspond to observed NOE pairs in the solution NMR. Only the distances that show significant deviations from the MD averages are given. As alluded to above, the largest differences are found in the separation between the central and the outermost strands of the β-sheet. The two distances of 6–7 Å calculated in the simulation are beyond the normally accepted range for NOE detection. A problem with the force field or the preparation of the system could be indicated. However, it is also possible that the protein is exploring the expanded phase of a low-frequency "breathing mode", and the separations may decrease at later times in the simulation.[34]

(C) Fluctuations. The overall mobility of the different atoms during an MD simulation can be expressed as their RMS fluctuations, $\langle \Delta r^2 \rangle^{1/2} = \langle (r_i - \langle r_i \rangle)^2 \rangle^{1/2}$, computed over the averaging period. An examination of the accumulated average atomic fluctuations as the time span of their evaluation increases shows, as expected, a monotonic increase for about 40 ps that levels toward a plateau after ca. 50 ps. These fluctuations can be compared to the average movement observed in the crystallographic determination as expressed in the B thermal factors. Crystallographic RMS fluctuations can then be derived via the relation $\langle \Delta r^2 \rangle^{1/2} = (3B/8\pi^2)^{1/2}$ from the B-values.[35] Figure 8 compares the RMS fluctuations calculated during the last 25 ps of the simulation with the fluctuations derived from the thermal factors.[22]

(33) Any missing hydrogen atoms in the X-ray and the MD structures were added by using the SYBYL program from TRIPOS Associates.
(34) Suezaki, Y.; Go, N. *Int. J. Pept. Protein Res.* **1975**, *7*, 333.
(35) Willis, B. T. M.; Pryor, A. W. *Thermal Vibrations in Crystallography*; Cambridge University Press: Cambridge, England, 1975.

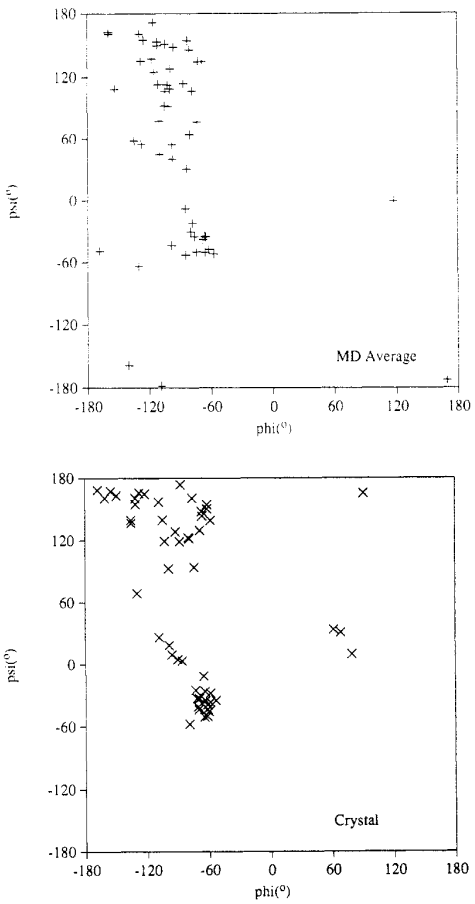

Figure 6. Ramachandran maps for the MD results and the crystal structure.

Table I. Average RMS Fluctuations (Å) for Different Atom Types

atoms	averaging time, ps		
	30–50	30–70	30–100
C^{α}	0.73	1.16	1.32
C^{β}	0.82	1.24	1.40
C^{γ}	0.90	1.30	1.50
C^{δ}	0.92	1.30	1.45
all protein	0.86	1.27	1.44
O^{water}	2.76	3.96	5.17

It can be seen from the plot that qualitative agreement in the width and location of the largest peaks is obtained. The most noticeable difference is the comparatively high fluctuations for the N-terminus in the simulation, which decrease until Cys-8 is reached. The first seven residues form a pendant chain whose increased mobility in solution can be attributed to the formation of a four-stranded β-channel with the N-terminal segments of neighboring molecules in the crystal.[22] The remaining qualitative differences reflect greater motion in the simulation for the side chains of Glu-10, Met-18, Asp-27, Lys-29, Glu-43, and Asn-45, which are more exposed to the solvent in the simulation than in the crystal structure.

The RMS fluctuations for the different atoms are correlated to their distances from the backbone of the protein. Table I lists the average RMS fluctuations for different carbon atoms for three averaging periods. The values obtained for the C^{δ} atoms have larger statistical uncertainties, since there are only 30 of these atoms in the protein. The fluctuations calculated in the initial 20 ps of the averaging period are comparable to those obtained in the simulations of aqueous trypsin–benzamidine during 19 ps (C^{α} = 0.52, C^{β} = 0.59, C^{γ} = 0.69, C^{δ} = 0.70, all = 0.68),[12] BPTI in "van der Waals water" for 25 ps (C^{α} = 0.54, C^{β} = 0.69, C^{γ} = 0.89, C^{δ} = 1.15, all = 0.78),[11a] and aqueous APP for 10 ps (C^{α} = 0.53, C^{β} = 0.62, C^{γ} = 0.73, C^{δ} = 0.79, all = 0.75).[9] However, the fluctuations calculated over the full averaging period of 70 ps are considerably larger than those reported by Levitt and Sharon for the final 105 ps of residues 2–56 of BPTI (C^{α} = 0.42, C^{β} = 0.50, C^{γ} = 0.54, C^{δ} = 0.67).[8] Greater experience is needed to ascertain if these differences are associated more with the proteins, the force fields, or the details of the simulation procedures, though further comment on this issue is made below.

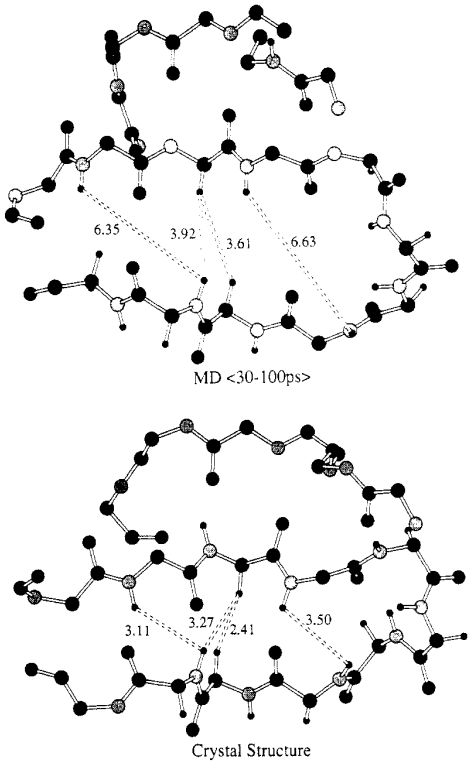

Figure 7. Backbone atoms of the β-sheet segments for the average MD structure and in the crsytal structure. Some interproton distances are shown.

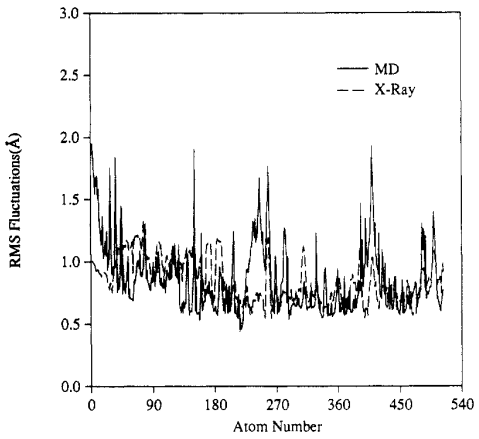

Figure 8. Comparison of RMS fluctuations from the MD calculation and from the crsytallographic *B*-factors.

(D) Hydrogen Bonding. Analyses of the intraprotein hydrogen bonding were carried out on the 700 coordinate sets saved during the last 70 ps of the MD simulation. The criteria used to define a hydrogen bond were purely geometric. A list of all potential donors and acceptors (hydrogens attached to heteroatoms and the heteroatoms themselves) was generated at the beginning of the analysis. For each coordinate set, every potential donor–acceptor

DOCKET ALARM

Explore Litigation Insights

Docket Alarm provides insights to develop a more informed litigation strategy and the peace of mind of knowing you're on top of things.

Real-Time Litigation Alerts

Keep your litigation team up-to-date with **real-time alerts** and advanced team management tools built for the enterprise, all while greatly reducing PACER spend.

Our comprehensive service means we can handle Federal, State, and Administrative courts across the country.

Advanced Docket Research

With over 230 million records, Docket Alarm's cloud-native docket research platform finds what other services can't. Coverage includes Federal, State, plus PTAB, TTAB, ITC and NLRB decisions, all in one place.

Identify arguments that have been successful in the past with full text, pinpoint searching. Link to case law cited within any court document via Fastcase.

Analytics At Your Fingertips

Learn what happened the last time a particular judge, opposing counsel or company faced cases similar to yours.

Advanced out-of-the-box PTAB and TTAB analytics are always at your fingertips.

API

Docket Alarm offers a powerful API (application programming interface) to developers that want to integrate case filings into their apps.

LAW FIRMS
Build custom dashboards for your attorneys and clients with live data direct from the court.

Automate many repetitive legal tasks like conflict checks, document management, and marketing.

FINANCIAL INSTITUTIONS
Litigation and bankruptcy checks for companies and debtors.

E-DISCOVERY AND LEGAL VENDORS
Sync your system to PACER to automate legal marketing.